Vol 42, No 2 (2025): October 2025

Jurnal Penelitian Pendidikan

https://journal.unnes.ac.id/journals/JPP

Dose Analysis in Boron Neutron Capture Therapy on Prostate Cancer using Phits Program Version 3.32

Rio Agustian Gilang Fernando[1]*, Pratiwi Dwijananti[1], Masturi[1] , Sunarno[1], Yohannes Sardjono[2]

[1]Universitas Negeri Semarang, Indonesia
[2]Pusat Riset Teknologi Keselamatan, Metrologi dan Mutu Nuklir
Organisasi Riset Tenaga Nuklir Badan Riset dan Inovasi Nasional

*Corresponding Author: rioagustiangf@gmail.com

Abstract

Prostate cancer is the second most common cancer in male worldwide. Boron Neutron Capture Therapy (BNCT) offers cancer treatment with minimum side effects. BNCT is radiation therapy that uses the 10B isotope and neutron beams which can selectively destroy tumor cells. The resulting radiation dose cannot be measured directly, so a computational method is needed to calculate the dose. The aim of this research is to determine the effective boron concentration, determine the optimal direction of irradiation, and determine the duration of irradiation time at an effective boron concentration for BNCT of prostate cancer. The computational method used is the Monte Carlo method with PHITS Version 3.32 software. The phantom used is an adult male ORNL phantom. The type of prostate cancer modeled is adenocarcinoma with an intermediate risk group. The neutron source is a 30 MeV cyclotron. Variations in 10B concentrations used were 100, 110, 120, 130, 140, and 150 μg/g boron/cancer tissue. The variations in direction used are: anterior-posterior, lateral-anterior oblique, and left-lateral. This study yield that the effective boron concentration used for BNCT in prostate cancer is 150 μg/g boron/cancer tissue. The most optimal radiation direction for BNCT of prostate cancer is the anterior-posterior direction. The duration of irradiation time required for a boron concentration of 150 μg/g boron/cancer tissue is 1 hour 16 minutes 10 seconds.

Keywords: BNCT, dosimetry, PHITS, prostate cancer

INTRODUCTION

Prostate cancer is the second most common cancer in male worldwide (Sung et al., 2021). In 2020, the incidence of prostate cancer in the world was 7.3% with a death rate of 3.8%. The incidence of prostate cancer reached 14.1% with mortality reaching 6.8% in male cases. In Indonesia there are 13,130 new cases of prostate cancer in 2022 with deaths reaching 4,860 people (Global Cancer Observatory, 2022). There are several common cancer treatment options, such as: chemotherapy, radiotherapy and surgery (Riis, 2020). These methods have drawback such as radiation in radiotherapy which can affect surrounding healthy tissue. Surgery generally only removes parts infected with malignant cells with a diameter of >0.5 cm, but smaller cancers are difficult to detect and remove (Marotta et al., 2020). Chemotherapy causes side effects such as fatigue, nausea, vomiting, and hair loss (Altun & Sonkaya, 2018). Based on these disadvantages, a method with fewer side effects was developed, namely the Boron Neutron Capture Therapy (BNCT) (Skwierawska et al., 2022).

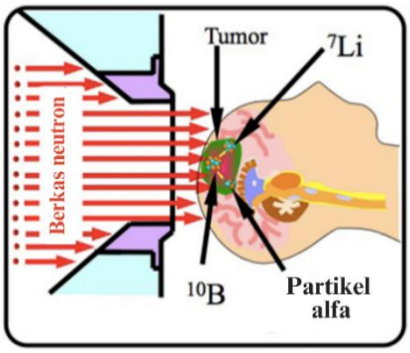

Figure 1. BNCT mechanism

BNCT is radiation therapy that uses ^{10}B isotopes and neutron beams (Sajad et al., 2022). BNCT can selectively destroy tumor cells because the neutron beam can specifically react in cells containing ^{10}B (Skwierawska et al., 2022). BNCT is based on a thermal neutron capture reaction with the isotope ^{10}B, which produces alpha particles and lithium-7 (Malouff et al., 2021). The Linear Energy Transfer (LET) of alpha particles (196 keV/µm) and 7Li nuclei (162 keV/µm) is quite high and has a limited penetration distance. The penetration distance of these particles is as long as the diameter of a single cell. The use of short-range radiation ensures that adjacent normal tissue is protected from radiation damage (Hsu et al., 2023). BNCT treatment is illustrated in Figure 1.

The targeting ability of BNCT is influenced by the dose of ^{10}B used for therapy (Cheng et al., 2022). The absorbed radiation dose cannot be measured directly, so the Monte Carlo computational method is used (Liang et al., 2020). The PHITS program is an application of the Monte Carlo method which allows creating artificial tissue models, cancer, and calculating absorbed dose (Sato et al., 2018). In this study, an analysis of the dose of prostate cancer therapy with BNCT was carried out using the PHITS version 3.32 program.

METHOD

This research was conducted from June 2023 to May 2024 at the Research Center for Nuclear Safety, Metrology, and Quality Technology, Nuclear Energy Research Organization, National Research and Innovation Agency (PRTKMMN ORTN BRIN). The hardware used is a laptop with specifications: Intel(R) Celeron(R) N4500 processor, 4 GB RAM, and Windows 11, 64-bit operating system. The software used are: PHITS version 3.32, Notepad++ v7.8.4, Ghostscript, Microsoft Word 2021, Microsoft Excel 2021.

The independent variables in this study are the direction of radiation and boron concentration in cancer. The irradiation directions used are anterior-posterior (AP), left-anterior oblique (LAO), and left-lateral (LLAT) (Figure 2). The boron concentrations used in this study were 100, 110, 120, 130, 140, and 150 µg/g boron/cancer tissue. The dependent variables in this study were total dose rate and irradiation time. The control variables in this study were BSA parameters, geometric size of prostate cancer, and tissue materials.

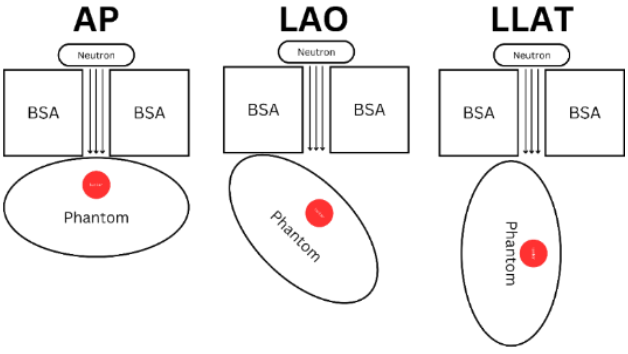

Figure 2. Irradiation direction for: AP, LAO, and LLAT

Geometry modeling is based on the Oak Ridge National Laboratory (ORNL) phantom model of adult male. The Organs at Risk (OAR) created in this study were the skin, bladder, testicles, large intestine, small intestine, femur head, pelvic bone, and genitals (Jang et al., 2021). The prostate cancer modeled is stage IIB prostate cancer which is classified in the intermediate category based on the Guidelines for radiotherapy of prostate cancer (2020 edition) (Li, Li, et al., 2021). The type of cancer modeled is adenocarcinoma. Prostate cancer usually presents with multifocal foci, so the target volume should include the entire prostate. In this

study, gross tumor volume (GTV) was chosen for the entire prostate, clinical target volume (CTV) of 1.0 cm covering the GTV, and planning target volume (PTV) of 0.7 cm covering the PTV. The ellipsoid equation is used in modeling the prostate (Stabin, 1994).

$$(1)\quad \left(\frac{x}{1{,}54}\right)^2 + \left(\frac{y+4{,}50}{1{,}54}\right)^2 + \left(\frac{z-2{,}93}{1{,}54}\right)^2 \leq 1$$

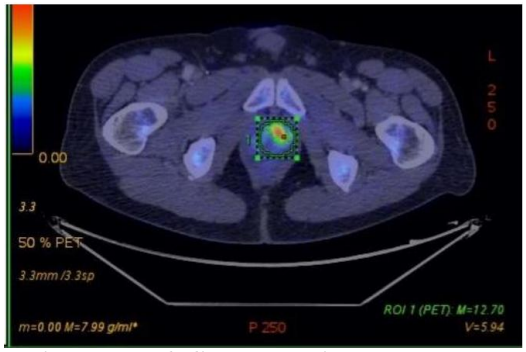

Figure 3. ^{18}F choline PET-CT in prostate cancer

From Equation 1 it can be seen that the prostate has a spherical geometry with a radius of 1.54 cm and is located at coordinates (0, -4.50, 2.93). As a reference, prostate cancer PET image data was taken from research conducted by Alshemeili (2020) in Figure 3.

Phantom materials data was taken from the Pacific Northwest National Laboratory (PNNL) (Detwiler et al., 2021) and the International Commission on Radiological Protection (ICRP) (Menzel et al., 2009). The composition of the genitals, bladder and prostate gland is the same as the composition of the soft tissues. The materials of the cancer were taken from the research result of Maughan et al. (1997).

The total dose rate is expressed as the total components of each dose rate multiplied by the appropriate weighting factor for each dose rate component (Li, Jiang, et al., 2021). The weighting factor for the dose of: nitrogen, photons and fast neutrons, is called Relative Biological Effectiveness (RBE). The weighting factor for boron dose is called Compound Biological Effectiveness (CBE). The weighting factors used in this study were 3.2 for nitrogen dose and fast neutron dose, and 1.0 for photon dose. For boron dose, a weighting factor of 3.8 is used for cancer tissue (Koivunoro et al., 2019) and 1.3 for healthy tissue (Schwint et al., 2020). The total dose can be calculated using equation 2.

$$(2)\quad \dot{D}_T = \left(w_B \dot{D}_B\right) + \left(w_p \dot{D}_p\right) + \left(w_n \dot{D}_n\right) + \left(w_\gamma \dot{D}_\gamma\right)$$

where $\dot{D_T}$ is the total dose rate (Gy/s), w_B is the boron weight factor, w_γ is the photon weight factor, w_p is the nitrogen weight factor, and w_n is the fast neutron weight factor.

Irradiation time can be calculated using equation 3.

$$(3)\quad t = \frac{D_{minimal}}{\dot{D_T}_{GTV}}$$

Where, t is the irradiation time (s), $D_{minimal}$ is the minimum dose of cancer damage, and $\dot{D_T}_{GTV}$ is the total tissue dose rate at GTV (Gy/s). Prostate cancer is modeled based on the Guidelines for radiotherapy of prostate cancer (Li, Li, et al., 2021), which is included in the intermediate risk group category. The dose used to treat intermediate risk group prostate cancer is 76-80 Gy. In this study, the minimum cancer damage dose used was 76 Gy.

The absorbed dose is obtained from the product of the dose rate with the irradiation time (Cember & Johnson, 2009).

$$(4)\quad D = \dot{D_T} \times t \qquad (3)$$

Where D is the absorbed dose (Gy), $\dot{D_T}$ is the total tissue dose rate (Gy/s), and t is the irradiation time (s).

The effective dose is the tissue-weighted sum of the equivalent doses in all specified tissues and organs of the body (Petoussi-Henss et al., 2010).

$$E = \sum_i w_i D_i \quad (4)$$

Where E is the effective dose (Sv), D_i is the equivalent dose to the tissue (Gy), w_i is the tissue weight factor. Tissue weight factors are taken from ICRP publication 103 (ICRP, 2007).

RESULTS AND DISCUSSION

The geometry of the phantom can be seen in Figure 4. The resulting phantom image can differ according to the selected coordinates. Figure 4 is a phantom image for a height of 82.93 cm from the base of the leg. The selection of these values is based on the center point of the GTV geometry.

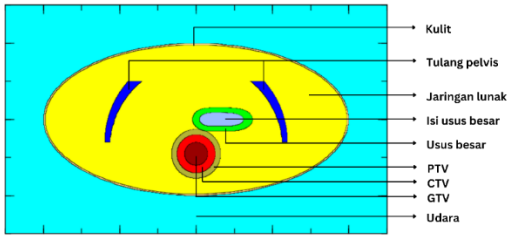

Figure 4. Phantom geometry

The BSA output obtained can be seen in Table 1. The filter and shielding materials used are: fast neutron filter (CaF_2) 12 cm, thermal neutron filter (B_4C) 0.3 cm, gamma shielding (Pb) 5 cm, and neutron shielding (borated paraffin) 3 cm. From the simulation results that have been obtained, all parameters recommended by the IAEA have been fulfilled.

Tabel 1. BSA output

Parameter	IAEA recommendation	Output result
$\phi_{epi}\ (n/cm^2s)$	$> 1.0 \times 10^9$	1.48×10^9
$\dot{D}_f/\phi_{epi}\ (Gy - cm^2/n)$	$< 2.0 \times 10^{-12}$	1.12×10^{-12}
$\dot{D}_\gamma/\phi_{epi}(Gy - cm^2/n)$	$< 2.0 \times 10^{-12}$	1.48×10^{-12}
ϕ_{th}/ϕ_{epi}	< 0.05	0.03
J/ϕ_{epi}	> 0.7	1.61

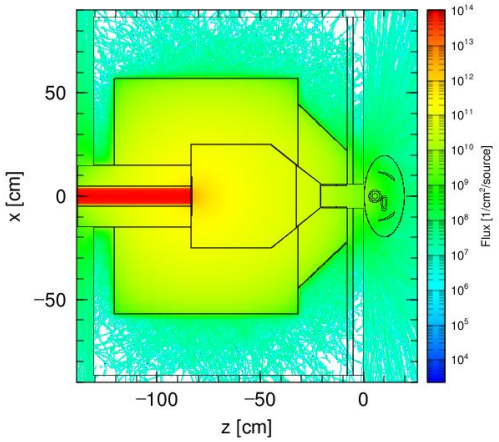

Figure 5. Particle Trajectory

The particle trajectories in the BSA and phantom can be seen in Figure 5. The distance between the BSA collimator and the skin surface is 0 cm. The considered particle trajectories are set for all particle types.

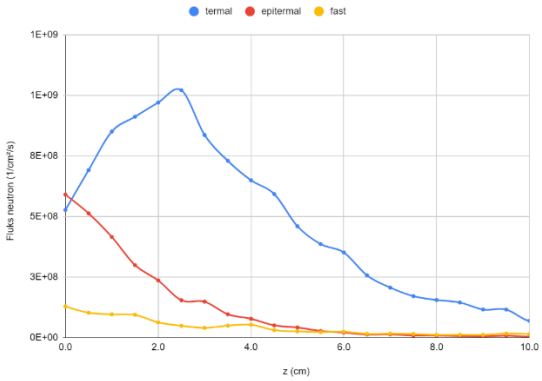

Figure 6. Neutron flux in phantom

In Figure 6, the highest thermal neutron flux was measured at a depth of 2.5 cm from the skin surface with a value of 1.02×10^9 neutrons.cm^{-2}s^{-1}. The highest epithermal neutron flux was measured at a depth of 0 cm from the skin surface with a value of 5.90×10^9 neutrons.cm^{-2}s^{-1}. The highest fast neutron flux was measured at a depth of 0 cm from the skin surface with a value of 1.29×10^8 neutrons.cm^{-2}s^{-1}.

The thermal neutron flux is 5.27×10^8 neutron.cm^{-2}s^{-1} at a depth of 0 cm from the skin surface and increases to 1.02×10^9 neutron.cm^{-2}s^{-1} at a depth of 2.5 cm. The increase in thermal neutron flux is due to the moderation of epithermal neutrons. Epithermal neutrons interacting with tissue will reduce the kinetic energy of the epithermal neutrons. This causes neutrons that were previously included in the epithermal neutron category to enter the thermal neutron category, which causes the thermal neutron flux to increase.

The total dose rate can be seen in Figure 7, Figure 8, and Figure 9.

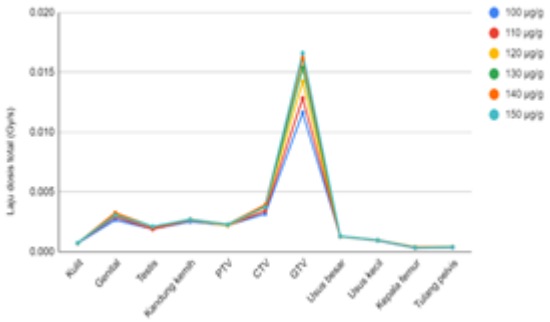

Figure 7. Total dose rate AP

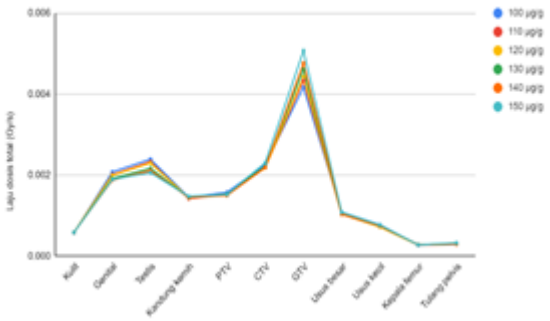

Figure 8. Total dose rate LAO

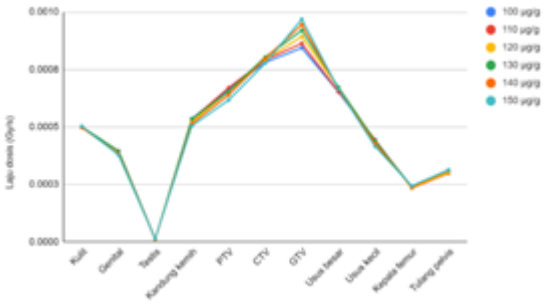

Figure 9. Total dose rate LLAT

In the AP irradiation direction, the highest total dose rate is received by GTV followed by CTV. This is because the highest concentration of ^{10}B is in the GTV region, while the concentration of ^{10}B in the CTV is half that of the GTV. The genital organs receive a relatively high dose rate due to their location relatively close to the BSA collimator. Other OARs that are deeper, such as: the large intestine, small intestine, femur head, and pelvis, receive a smaller dose rate.

The dose rate in OAR for the LAO radiation direction is quite high for the genital, testicles and urinary bladder. The direction of LLAT irradiation produces high dose rates in all organs except the testicles. This is because the irradiation geometry made the cancer distance further away from the BSA.

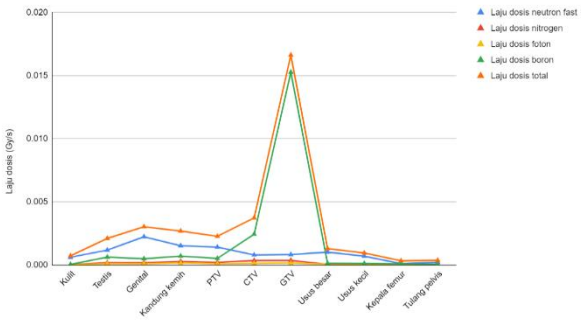

Figure 10. Dose rate per component AP

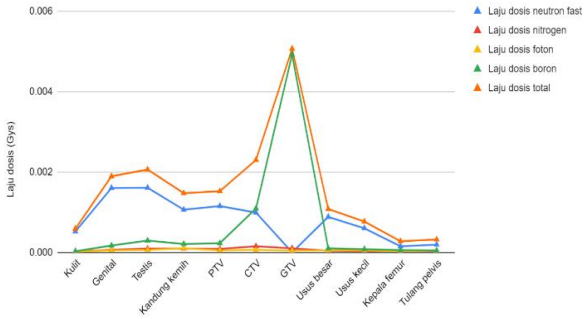

Figure 11. Dose rate per component LAO

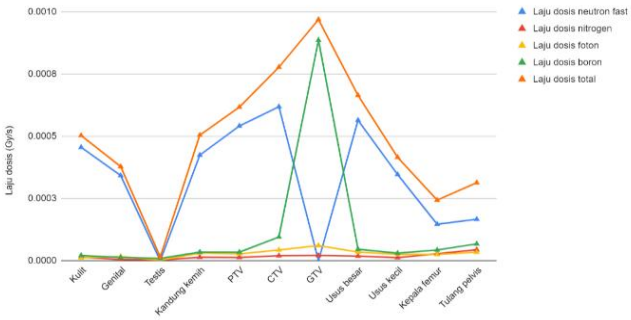

Figure 12. Dose rate per component LLAT

Figure 10 is a graph of the dose rate in the OAR for a ^{10}B concentration of 150 µg/g in the AP irradiation

direction. The dose rate component that is significant in the total dose rate of GTV is the boron component. The fast neutron dose rate component is more dominant in the genital organs because the genital is located at a depth of 0.2-10 cm where the fast neutron flux is still quite high. In the LAO and LLAT irradiation directions (Figure 11 and Figure 12), the fast neutron dose is a significant component of the total dose rate. This high dose is caused by the distance between the cancer and the neutron source being too far, causing the neutrons to interact with more tissue before reaching the cancer.

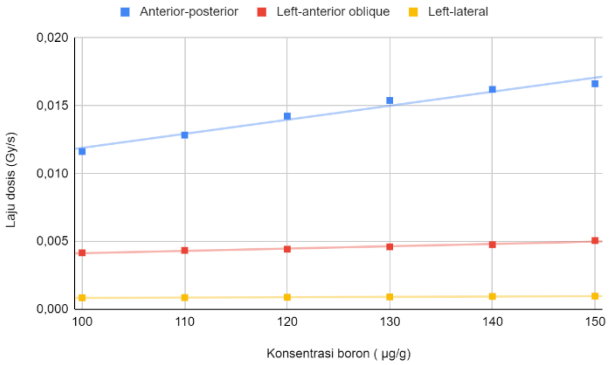

Figure 13. Dose rate in GTV

As can be seen in Figure 13, the result show a linear relation between ^{10}B concentration and dose rate at GTV. The greater the concentration of ^{10}B used, the greater the dose rate value. In the AP radiation direction, a ^{10}B concentration of 100 µg/g produces the smallest dose rate with the value 1.16×10^{-2} Gy/s. A ^{10}B concentration of 150 µg/g produced the largest dose rate with the value 1.66×10^{-2} Gy/s. In the LAO irradiation direction, a ^{10}B concentration of 100 µg/g produced the smallest dose rate with the value 4.17×10^{-4} Gy/s. A ^{10}B concentration of 150 µg/g produced the largest dose rate with the value 5.07×10^{-4} Gy/s. In the LLAT irradiation direction, a ^{10}B concentration of 100 µg/g produced the smallest dose rate with the value 8.44×10^{-4} Gy/s. A ^{10}B concentration of 150 µg/g produced the largest dose rate value, namely 9.68×10^{-4} Gy/s. The AP irradiation direction has the largest dose rate of the three irradiation directions.

The irradiation time for each ^{10}B concentration and each irradiation direction can be observed in Figure 14.

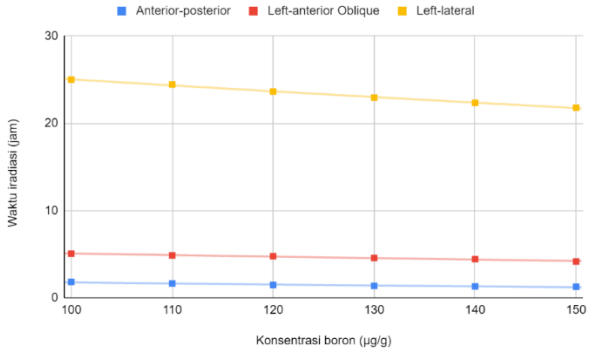

Figure 14. Irradiation time

In the AP irradiation direction, a ^{10}B concentration of 100 µg/g required the longest irradiation time, namely 1 hour 48 minutes 58 seconds. A ^{10}B concentration of 150 µg/g requires the shortest irradiation time, namely 1 hour 16 minutes 10 seconds. In the LAO irradiation direction, a ^{10}B concentration of 100 µg/g required the longest irradiation time with the value of 5 hours 4 minutes 6 seconds. A ^{10}B concentration of 150 µg/g required the shortest irradiation time with the value of 4 hours 9 minutes 53 seconds. In the direction of LLAT irradiation, a ^{10}B concentration of 100 µg/g requires the longest irradiation time with the value of 25 hours. A ^{10}B concentration of 150 µg/g required the shortest irradiation time with the value of 21 hours 48 minutes. The AP irradiation direction has the shortest irradiation time of the three irradiation directions. The ideal irradiation time is less than 1 hour (IAEA, 2023). The irradiation time will be faster if the concentration of ^{10}B is increased.

The location of the prostate organ, classified as deep in BNCT, means that the neutron flux is insufficient on the way to the target. Low neutron flux makes the dose rate also low. Another thing that can be used to increase the irradiation time is to increase the thermal neutron flux in the GTV at a depth of 3.96-

7.04 cm from the skin surface. This can be done by increasing the average flux of epithermal neutrons, so that the dose received by the cancer becomes higher. Regarding depth, irradiation can be performed transperitoneally (Figure 15). Using this approach, a sufficient neutron beam can be achieved (Takahara et al., 2022).

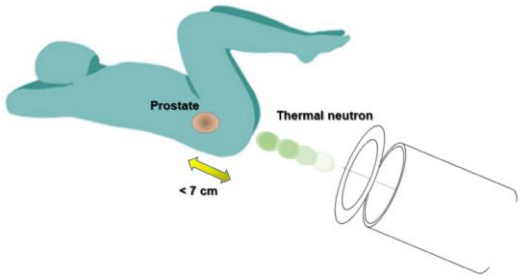

Figure 15. Transperitoneal irradiation

Histogram showing the equivalent dose received by OAR can be seen in Figure 16, Figure 17, and Figure 18. The graph also shows the relation between the ^{10}B concentration and the equivalent dose of each OAR in general. The greater the ^{10}B concentration, the smaller the equivalent dose received by the OAR.

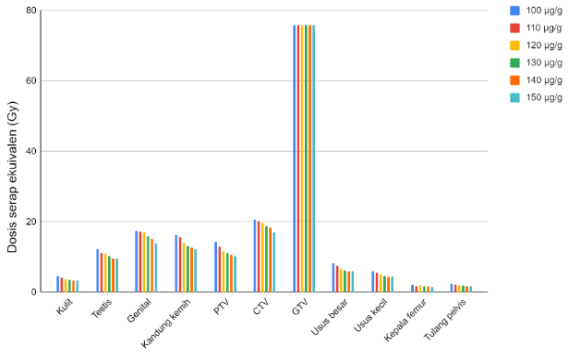

Figure 16. Equivalent dose OAR AP

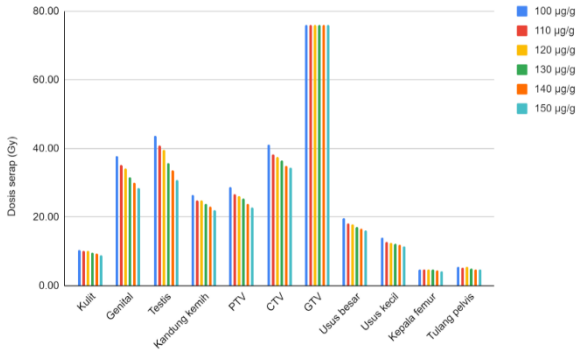

Figure 17. Equivalent dose OAR LAO

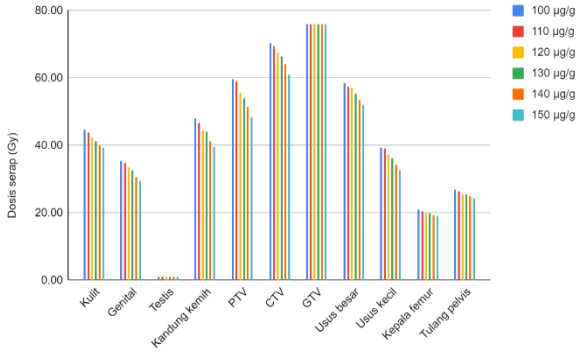

Figure 18. Equivalent dose OAR LLAT

The equivalent dose values that have been obtained are then compared with the equivalent dose tolerance limits for each OAR in Table 2. The ^{10}B concentration that is effective for BNCT therapy for prostate cancer is the ^{10}B concentration that provides the minimum equivalent dose to the OAR, but has the shortest irradiation time.

Tabel 2. OAR dose limits

No	OAR	Limit dose Gy)
1	Skin	14,4[b]
2	Genital	14[b]
3	Testicles	10[b]
4	Bone	30[a]
5	Femur head	14[a]
6	Urinary bladder	30[c]
7	Large intestine	11[a]
8	Small intestine	9,8[a]

a.)Cèfaro et al. (2013), b.)Emami (2013), c.) Arians et al. (2020)

Based on Table 2, in the direction of LAO irradiation there are several organs that exceed the tolerance limit, namely: testicles, genital, large intestine and small intestine. In the direction of LLAT irradiation, there are several organs that exceed the tolerance limit, namely: skin, genital, urinary bladder, large intestine, small intestine and femur head. The main goal of radiotherapy is to deliver a dose of radiation to the tumor to kill cancer cells without damaging the surrounding healthy organs and tissues (Zarepisheh et al., 2022). In this study, LAO and LLAT for all boron concentrations were not effective for use as BNCT for prostate cancer because many OARs received doses exceeding the threshold.

In the AP irradiation direction, it can be seen that the testicular organ receives an equivalent absorbed dose of 9.64 Gy, 9.65 Gy, and 10.32 Gy for ^{10}B concentrations of 150 µg/g, 140 µg/g, and 130 µg/g, respectively. consecutive. Referring to Table 2, only irradiation with ^{10}B concentrations of 150 µg/g and 140 µg/g is still below the testicles dose limit. Concentrations lower than 140 µg/g result in the testicles receiving a dose of more than 10 Gy. If the testicles receive a dose of ≥ 10 Gy, the patient will experience oligospermia or azoospermia. Recovery from these effects depends on the total dose received (Cèfaro et al., 2013). The skin receives 3.34 Gy of radiation. Referring to the Regulation of the Head of the Nuclear Energy Supervisory Agency (BAPETEN) Number 6 of 2010 concerning Health Monitoring for Radiation Workers (BAPETEN, 2010), erythema appears if the skin receives a dose of 3 Gy. Erythema is redness of the skin as an inflammatory response to wounds caused by ionizing radiation (Abdlaty et al., 2021). The genital will experience erectile dysfunction if the genitals receive a dose of more than 14 Gy in one fraction. If the genital receive a dose of 13.85 Gy, this dose is still below 14 Gy (Cèfaro et al., 2013). The equivalent dose received by other OARs is still below the OAR dose limit.

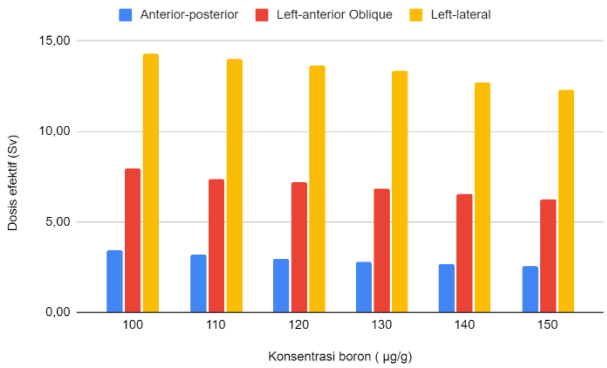

Figure 19. Effective dose AP, LAO, and LLAT

Effective dose can be seen in Figure 19. The three irradiation directions show the same trend, the higher the boron concentration used, the lower the effective dose. In the AP radiation direction, the largest effective dose was 3.41 Sv at a boron concentration of 100 µg/g, and the lowest effective dose was 2.54 Sv at a boron

concentration of 150 μg/g. In the LAO irradiation direction, the highest effective dose was 7.98 Sv at a boron concentration of 100 μg/g, and the lowest effective dose was 6.26 Sv at a boron concentration of 150 μg/g. In the LLAT irradiation direction, the highest effective dose was 14.28 Sv at a boron concentration of 100 μg/g, and the lowest effective dose was 12.30 Sv at a boron concentration of 150 μg/g.

The effective dose provides information regarding the possible health risks of a particular radiation procedure. The higher the effective dose value, the higher the possibility of health problems arising from radiation (Martin et al., 2020). The variation with the lowest effective dose is the AP irradiation direction with a boron concentration of 150 μg/g. This variation allows the destruction of cancer with the lowest absorbed dose at the OAR and the lowest possibility of health problems resulting from radiation.

CONCLUSION

Based on the analysis of boron dose in prostate cancer using the BNCT method, it has been concluded that the effective concentration of boron for this treatment is 150 μg/g of cancer tissue. The optimal radiation direction for BNCT in prostate cancer is the anterior-posterior direction. The required irradiation time for this boron concentration is 1 hour, 16 minutes, and 10 seconds.

ACKNOWLEDGMENTS

The author expresses his gratitude to all the contributors who assisted and supported the completion of this project. Special thanks go to the Research Center for Nuclear Safety, Metrology, and Quality Technology, Nuclear Energy Research Organization, National Research and Innovation Agency (PRTKMMN ORTN BRIN) for providing the opportunities to conduct this research, and to Prof. Ir. Yohannes Sardjono, APU from PRTKMMN ORTN BRIN for his guidance on the software used in this study.

REFERENCES

Abdlaty, R., Abbass, M. A., & Awadallah, A. M. (2021). High Precision Monitoring of Radiofrequency Ablation for Liver Using Hyperspectral Imaging. *Annals of Biomedical Engineering*, *49*(9), 2430–2440. https://doi.org/10.1007/s10439-021-02797-w

Altun, İ., & Sonkaya, A. (2018). The Most Common Side Effects Experienced by Patients Were Receiving First Cycle of Chemotherapy. *Iranian Journal of Public Health*, *47*(8), 1218–1219.

Arians, N., Häfner, M., Krisam, J., Lang, K., Wark, A., Koerber, S. A., Hommertgen, A., & Debus, J. (2020). Intrafractional vaginal dilation in anal cancer patients undergoing pelvic radiotherapy (DILANA) – a prospective, randomized, 2-armed phase-II-trial. *BMC Cancer*, *20*(1), 52. https://doi.org/10.1186/s12885-020-6547-7

BAPETEN. (2010). *Peraturan Kepala Badan Pengawas Tenaga Nuklir Nomor 6 Tahun 2010 Tentang Pemantauan Kesehatan Untuk Pekerja Radiasi*.

Cèfaro, G. A., Genovesi, D., & Perez, C. A. (2013). *Delineating Organs at Risk in Radiation Therapy*. Springer Milan. https://doi.org/10.1007/978-88-470-5257-4

Cember, H., & Johnson, T. E. (2009). *Introduction to Health Physics* (4th ed.). McGraw-Hill.

Cheng, X., Li, F., & Liang, L. (2022). Boron Neutron Capture Therapy: Clinical Application and Research Progress. *Current Oncology*, *29*(10), 7868–7886. https://doi.org/10.3390/curroncol29100622

Detwiler, R., McConn, R., Grimes, T., Upton, S., & Engel, E. (2021). *Compendium of Material Composition Data for Radiation Transport Modeling*. https://doi.org/10.2172/1782721

Emami, B. (2013). Tolerance of Normal Tissue to Therapeutic Radiation. *Reports of Radiotherapy and Oncology*, *1*(1), 35–48.

Global Cancer Obeservatory. (2022). *Cancer Today Gobocan 2022: Indonesia*. https://gco.iarc.who.int/media/globocan/factsheets/populations/360-indonesia-fact-sheet.pdf.

Hsu, C.-F., Liu, H.-M., Peir, J.-J., Liao, J.-W., Chen, K.-S., Chen, Y.-W., Chuang, Y.-J., & Chou, F.-I. (2023). Therapeutic Efficacy and Radiobiological Effects of Boric-Acid-Mediated BNCT in an Osteosarcoma-Bearing SD Rat Model. *Life*, *13*(2), 514. https://doi.org/10.3390/life13020514

IAEA. (2023). *Advances in Boron Neutron Capture Therapy*. International Atomic Energy Agency.

ICRP. (2007). The 2007 Recommendations of the International Commission on Radiological Protection. ICRP publication 103. *Annals of the ICRP*, *37*(2–4), 1–332. https://doi.org/10.1016/j.icrp.2007.10.003

Jang, H., Park, J., Artz, M., Zhang, Y., Ricci, J. C., Huh, S., Johnson, P. B., Kim, M.-H., Chun, M., Oh, Y.-T., Noh, O. K., & Park, H.-J. (2021). Effective Organs-at-Risk Dose Sparing in Volumetric Modulated Arc Therapy Using a Half-Beam Technique in Whole Pelvic Irradiation. *Frontiers in Oncology*, *11*. https://doi.org/10.3389/fonc.2021.611469

Koivunoro, H., Kankaanranta, L., Seppälä, T., Haapaniemi, A., Mäkitie, A., & Joensuu, H. (2019). Boron Neutron Capture Therapy for Locally Recurrent Head and Neck Squamous Cell Carcinoma: an Analysis of Dose Response and Survival. *Radiotherapy and Oncology*, *137*, 153–158. https://doi.org/10.1016/j.radonc.2019.04.033

Li, G., Jiang, W., Zhang, L., Chen, W., & Li, Q. (2021). Design of Beam Shaping Assemblies for Accelerator-Based BNCT With Multi-Terminals. *Frontiers in Public Health*, *9*. https://doi.org/10.3389/fpubh.2021.642561

Li, G., Li, Y., Wang, J., Gao, X., Zhong, Q., He, L., Li, C., Liu, M., Liu, Y., Ma, M., Wang, H., Wang, X., & Zhu, H. (2021). Guidelines for Radiotherapy of Prostate Cancer (2020 edition). *Precision Radiation Oncology*, *5*(3), 160–182. https://doi.org/10.1002/pro6.1129

Liang, Y., Muhammad, W., Hart, G. R., Nartowt, B. J., Chen, Z. J., Yu, J. B., Roberts, K. B., Duncan, J. S., & Deng, J. (2020). A General-purpose Monte Carlo Particle Transport Code Based on Inverse Transform Sampling for Radiotherapy Dose Calculation. *Scientific Reports*, *10*(1), 9808. https://doi.org/10.1038/s41598-020-66844-7

Malouff, T. D., Seneviratne, D. S., Ebner, D. K., Stross, W. C., Waddle, M. R., Trifiletti, D. M., & Krishnan, S. (2021). Boron Neutron Capture Therapy: A Review of Clinical Applications. *Frontiers in Oncology*, *11*. https://doi.org/10.3389/fonc.2021.601820

Marotta, C. B., Haber, T., Berlin, J. M., & Grubbs, R. H. (2020). Surgery-Guided Removal of Ovarian Cancer Using Up-Converting Nanoparticles. *ACS Applied Materials & Interfaces*, *12*(43), 48371–48379. https://doi.org/10.1021/acsami.0c14983

Martin, C. J., Harrison, J. D., & Rehani, M. M. (2020). Effective Dose from Radiation Exposure in Medicine: Past, Present, and Future. *Physica Medica*, *79*, 87–92. https://doi.org/10.1016/j.ejmp.2020.10.020

Maughan, R. L., Chuba, P. J., Porter, A. T., Ben-Josef, E., & Lucas, D. R. (1997). The Elemental Composition of Tumors: Kerma Data for Neutrons. *Medical Physics*, *24*(8), 1241–1244. https://doi.org/10.1118/1.598144

Menzel, H.-G., Clement, C., & DeLuca, P. (2009). ICRP Publication 110. Realistic reference phantoms: an ICRP/ICRU joint effort. A report of adult reference computational phantoms. *Annals of the ICRP*, *39*(2), 1–164. https://doi.org/10.1016/j.icrp.2009.09.001

Petoussi-Henss, N., Bolch, W. E., Eckerman, K. F., Endo, A., Hertel, N., Hunt, J., Pelliccioni, M., Schlattl, H., & Zankl, M. (2010). Conversion Coefficients for Radiological Protection Quantities for External Radiation Exposures. *Annals of the ICRP*, *40*(2–5), 1–257. https://doi.org/10.1016/j.icrp.2011.10.001

Riis, M. (2020). Modern Surgical Treatment of Breast Cancer. *Annals of Medicine and Surgery*, *56*, 95–107. https://doi.org/10.1016/j.amsu.2020.06.016

Sajad, K., Elnaz, E., Dariush, S., Darki, S. Y., & Marzieh, K. (2022). Boron Neutron Capture Therapy for The Treatment of Lung Cancer and Assessment of Dose Received by Organs at Risk. *Archives of Pathology and Clinical Research*, *6*(1), 027–031. https://doi.org/10.29328/journal.apcr.1001032

Sato, T., Iwamoto, Y., Hashimoto, S., Ogawa, T., Furuta, T., Abe, S., Kai, T., Tsai, P.-E., Matsuda, N., Iwase, H., Shigyo, N., Sihver, L., & Niita, K. (2018). Features of Particle and Heavy Ion Transport Code System (PHITS) Version 3.02. *Journal of Nuclear Science and Technology*, *55*(6), 684–690. https://doi.org/10.1080/00223131.2017.1419890

Schwint, A. E., Monti Hughes, A., Garabalino, M. A., Santa Cruz, G. A., González, S. J., Longhino, J., Provenzano, L., Oña, P., Rao, M., Cantarelli, M. de los Á., Leiras, A., Olivera, M. S., Trivillin, V. A., Alessandrini, P., Brollo, F., Boggio, E., Costa, H., Ventimiglia, R., Binia, S., … Santa Cruz, I. S. (2020). Clinical Veterinary Boron Neutron Capture Therapy (BNCT) Studies in Dogs with Head and Neck Cancer: Bridging the Gap between Translational and Clinical Studies. *Biology*, *9*(10), 327. https://doi.org/10.3390/biology9100327

Skwierawska, D., López-Valverde, J. A., Balcerzyk, M., & Leal, A. (2022). Clinical Viability of Boron Neutron Capture Therapy for Personalized Radiation Treatment. *Cancers*, *14*(12), 2865. https://doi.org/10.3390/cancers14122865

Stabin, M. G. (1994). A Model of the Prostate Gland for Use in Internal Dosimetry. *Journal of Nuclear Medicine : Official Publication, Society of Nuclear Medicine*, *35*(3), 516–520.

Sung, H., Ferlay, J., Siegel, R. L., Laversanne, M., Soerjomataram, I., Jemal, A., & Bray, F. (2021).

Global Cancer Statistics 2020: GLOBOCAN Estimates of Incidence and Mortality Worldwide for 36 Cancers in 185 Countries. *CA: A Cancer Journal for Clinicians*, *71*(3), 209–249. https://doi.org/10.3322/caac.21660

Takahara, K., Miyatake, S., Azuma, H., & Shiroki, R. (2022). Boron Neutron Capture Therapy for Urological Cancers. *International Journal of Urology*, *29*(7), 610–616. https://doi.org/10.1111/iju.14855

Zarepisheh, M., Hong, L., Zhou, Y., Huang, Q., Yang, J., Jhanwar, G., Pham, H. D., Dursun, P., Zhang, P., Hunt, M. A., Mageras, G. S., Yang, J. T., Yamada, Y. (Josh), & Deasy, J. O. (2022). Automated and Clinically Optimal Treatment Planning for Cancer Radiotherapy. *INFORMS Journal on Applied Analytics*, *52*(1), 69–89. https://doi.org/10.1287/inte.2021.1095